ISSN 1054-660X, Laser Physics, 2011, Vol. 21, No. 7, pp. 1329–1335.

Pulse Fidelity Control in a 20-μJ Sub-200-fs Monolithic Yb-Fiber Amplifier[1]

A. Fernández[a, *], L. Zhu[a], A. J. Verhoef[a], D. Sidorov-Biryukov[a, b], A. Pugzlys[a], A. Galvanauskas[c], F. Ö. Ilday[d], and A. Baltuška[a]

[a] *Institut für Photonik, Technische Universität Wien, Gusshausstrasse 27-29/387, 1040 Wien, Austria*
[b] *International Laser Center, Moscow State University, Moscow, 119992 Russia*
[c] *Center for Ultrafast Optical Science, University of Michigan, Ann Arbor, MI 48109-2099, USA*
[d] *Department of Physics, Bilkent University, Cankaya, Ankara 06800, Turkey*
*e-mail: almadelc@mail.tuwien.ac.at

Received October 2, 2010; in final form, January 27, 2011; published online June 4, 2011

Abstract—We discuss nonlinearity management versus energy scalability and compressibility in a three-stage monolithic 100-kHz repetition rate Yb-fiber amplifier designed as a driver source for the generation and tunable parametric amplification of a carrier-envelope phase stable white-light supercontinuum.

DOI: 10.1134/S1054660X11130111

1. INTRODUCTION

Compact and environmentally stable high-energy ultrashort-pulse laser sources have many applications. Examples include biomedical applications (e.g., ophthalmology, biomedical imaging), laser micromachining, index modification in transparent materials (waveguide writing), and frequency conversion. Fiber lasers offer big practical advantages over bulk solid-state laser systems. In terms of flexibility, compactness, reliability, cost effectiveness and turn-key operability, a fiber-based laser system is the preferred laser architecture. Moreover, thermal effects are reduced because fibers have a large surface to volume ratio and the waveguiding properties of fibers ensure good spatial mode quality. With the light guided in a fiber the system is less sensitive to misalignment but this great advantage of fiber laser has not yet been fully exploited and a considerable amount of free standing elements (grating stretcher, in-coupling optics), are commonly used. Parametric amplification is a powerful technique that has been used to achieve wavelength tunability outside the gain bandwidths of optical fiber amplifiers as well as to shorten the pulses generated directly from fiber amplifiers below 10 fs [1, 2]. For many applications in high field physics and attosecond science carrier envelope-phase (CEP) stable pulses are required. Ytterbium doped fiber amplifiers (YDFA) are very attractive scalable sources for seeding and pumping of CEP-stable difference frequency generation (DFG) optical parametric amplifiers (OPAs) [3, 4]. Generation of temporally compressible white light in bulk media for OPA seeding, requires high-fidelity sub-200-fs pulses to minimize the impact of non-instantaneous (e.g., Raman) nonlinearities [5]. Due to a large amount of higher-order linear and nonlinear dispersion [6–8], such pulses are difficult to obtain from YDFA, prompting the use of solid-state lasers for driving OPAs. Yb-doped fibers support broader bandwidths than their crystalline counterparts and using the scheme of chirped-pulse amplification (CPA) in combination with the use of large core specialty fibers YDFA delivering tens and even hundreds of micro-Joules have been demonstrated [9–11]. Realization of these systems requires a considerable amount of free standing components which is detrimental for system stability. Replacing the free-space stretcher optics by a fiber-stretcher is of key importance for achieving a robust turn-key alignment-free design. Compression of up to 100 m of single mode fiber (SMF) using a pair gratings has been demonstrated, in an approach that exploits compensation of self-phase modulation by third-order dispersion and it is known a nonlinear CPA (NLCPA) [9]. In another approach by the same group, better pulse compressibility was achieved by using a grism compressor instead of a grating compressor [12]. Although those systems used a fiber stretcher, the active media of the system were based on specialty fibers therefore such a setup still required a considerable amount of free space in-coupling optics. Recently a monolithic fiber amplifier delivering 170 fs pulses at ~4 μJ of pulse energy was reported. This system is based on the so called NLCPA and although short pulses are obtained, the pulse fidelity is strongly degraded with a considerably portion of the pulse energy in the pulse pedestal [13]. In many applications polarization maintaining (PM) fibers are required and therefore there is a lot of interest not only in having a monolithic fiber architecture but an environmentally stable linearly polarized system as well [14]. We have previously demonstrated a monolithic PM-YDFA that delivers sub-200-fs high fidelity pulses with energies of up to 9 μJ [4]. In this work we followed a differ-

[1] The article is published in the original.

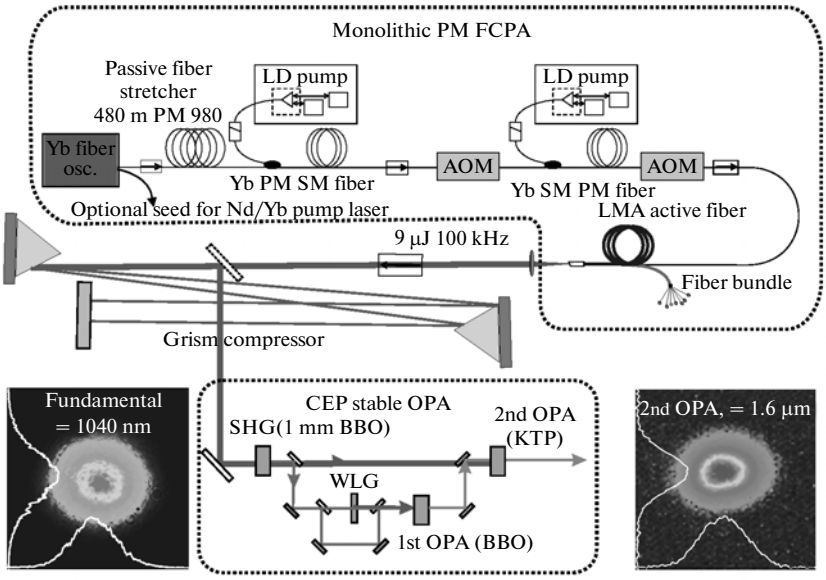

Fig. 1. Experimental layout of the monolithic fiber CPA and DFG OPA (for details see text). In the lower part far-field mode profiles of the FCPA output (left) and CEP-stable output of DFG OPA (right) are presented.

ent approach in which the amount of nonlinearities in the system are kept low. The pulses were stretched in ~480 m of PM SMF and re-compressed with a pair of grisms. Here we discuss in detail key design parameters that have to be taken in consideration for designing a high fidelity sub-200-fs monolithic YDFA and present an improved system that delivers up to 21 μJ with a dechirped pulse duration of ~187 fs.

2. EXPERIMENTAL SETUPS AND DISCUSSION

Two different experimental setups for the YDFA were investigated and will be discussed in detailed in this section. The experimental layout of the first YDFA system is shown in Fig. 1. Note that in the same figure we also show the layout of a type II collinear CEP stable OPA which will be discussed in detailed later on in this section. The YDFA system consists of a fiber oscillator, a stetcher unit consisting of ~480 m of PM SMF, two PM SMF preamplifiers and a PM large mode area (LMA) fiber amplifier. In order to keep nonlinearities low, in both preamplifiers 1.5 m of highly Yb-doped PM SMF from Nufern (PM-YDF-HI) is used as an active medium. After the first amplification stage a fiber pigtailed acousto-optic modulator (AOM) was used to reduce the repetition rate to 100 kHz. Another fiber pigtailed AOM was used after the second amplification stage to suppress amplified spontaneous emission. Via a tapered fiber, the preamplified pulses are launched into the final LMA fiber amplifier. This last amplification stage consists of 3 m of Yb-doped PM LMA double clad fiber (PLMA-YDF-30/250 from Nufern) and a seed-pump combiner (PASA-YD-30/250-7 × 1 from Nufern). The LMA has a core diameter of 30 μm, corresponding to a mode field diameter of ~625 μm^2. The output is taken after a free space isolator with a transmission of ~90%. The far field beam profile of the monolithic fiber CPA output is shown in the left inset of Fig. 1.

In order to find the optimal working conditions for the preamplifier stages the accumulated spectral phase of the pulse after the stretcher, and after each of the first two PM SMF preamplifier stages was measured using second harmonic generation frequency resolved optical gating (SHG FROG). The pulses were compressed in a negative dispersion compressor based on a pair of grisms, each being an assembly of an F2 glass prism and a 1480 lines/mm reflection grating. The compressor efficiency is ~45%. The same measurements were performed for two different oscillator types: an all normal dispersion fiber (ANDi) oscillator as described in [15] and a similariton type fiber oscillator. No significant spectral phase distortion was observed after the stretcher and the first amplification stage. Spectral phase distortions start to be relevant after the second amplification stage.

The measured spectral phases for different output energy levels after the second amplification stage are shown in Figs. 2a and 2b for the ANDi oscillator and the similariton-type oscillator respectively. It can be seen that with increasing intensity the spectral region where the spectral phase remains approximately flat decreases due to bending of the phase at the edges of the spectrum. This effect is more pronounced on the shorter wavelength side of the spectrum, which may be due to enhanced self phase modulation in the presence

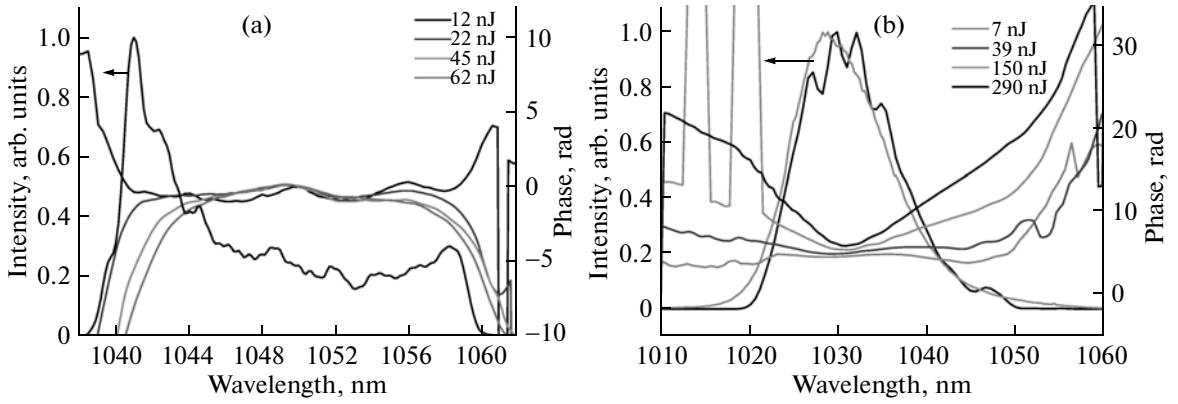

Fig. 2. Measured spectral phases for different energies of the recompressed pulses after the second amplification stage. Two different master oscillators as seed sources are compared: (a) a standard ANDi oscillator and (b) a similariton type oscillator.

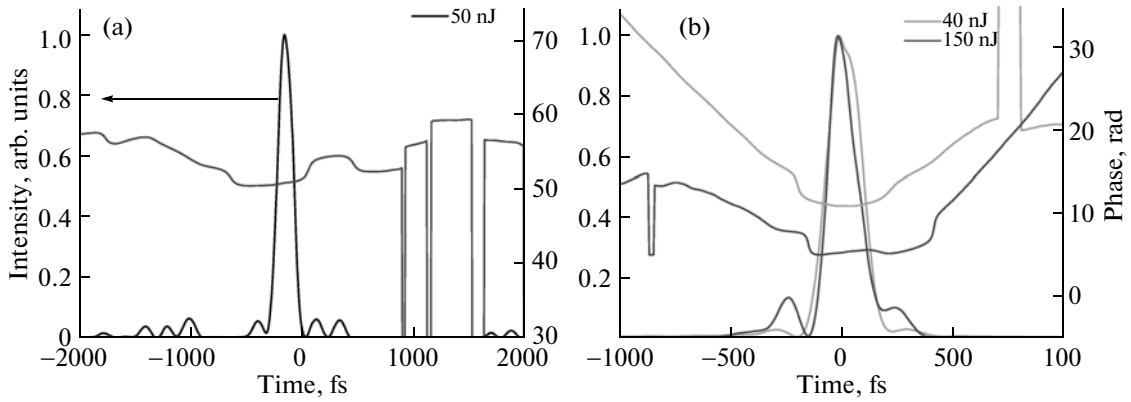

Fig. 3. Retrieved temporal phases and temporal profile of the recompressed pulses after the second amplification stage. Two different master oscillators as seed sources are compared: (a) a standard ANDi oscillator and (b) a similariton type oscillator.

of higher gain. Figure 3a shows the retrieved pulse and its corresponding temporal phase for a pulse energy of 50 nJ after the second amplifier stage using the ANDi oscillator as a seed source. As can be seen from this figure the pulse quality is very poor with a considerable part of the energy lying in satellite pulses. SHG FROG measurements of the output pulses after the LMA amplification stage show a similar situation. The pulses delivered by the ANDi oscillator turned out to be not suitable for seeding the monolithic YDFA. In [16] a slightly modified oscillator configuration with two output ports has been proposed to obtain cleaner pulses, which might be better suited for seeding YDFA. As shown in Fig. 2b, when using the similariton-type oscillator as a seed source bending of the spectral phase at the edges of the spectrum with increased pulse energy was also observed. Figure 3b shows the retrieved pulses and their corresponding temporal phases for 40 and 150 nJ pulses. As can be seen pulse compressibility has dramatically improved compared to the previous case.

By using the similariton-type oscillator to seed the monolithic YDFA up to 9 μJ pulses were obtained. These pulses were compressed down to sub-200-fs high fidelity pulses (see Fig. 4). In addition, by increasing the pump power of the final amplifier stage, the output pulse energy can be raised above 10 μJ. However, this energy is obtained at the expense of severe pulse splitting and this proved to be disadvantageous to driving the OPA. To overcome this limitation some key modifications to the YDFA seeded with the similariton-type oscillator were implemented: the length of the fiber stretcher was increased from 480 to 800 m and the 3 m of active PM LMA fiber was replaced by ~1.8 m of PM LMA fiber with a higher doping concentration (PLMA-YDF-30/250-HI from Nufern). A grism compressor with improved efficiency of ~55% consisting of bigger F2 glass prisms and bigger 1480 lines/mm gratings was used to compress the pulses. The experimental setup for this YDFA is shown in Fig. 5. In order to determine the maximum pulse energy that can be attained with the new YDFA con-

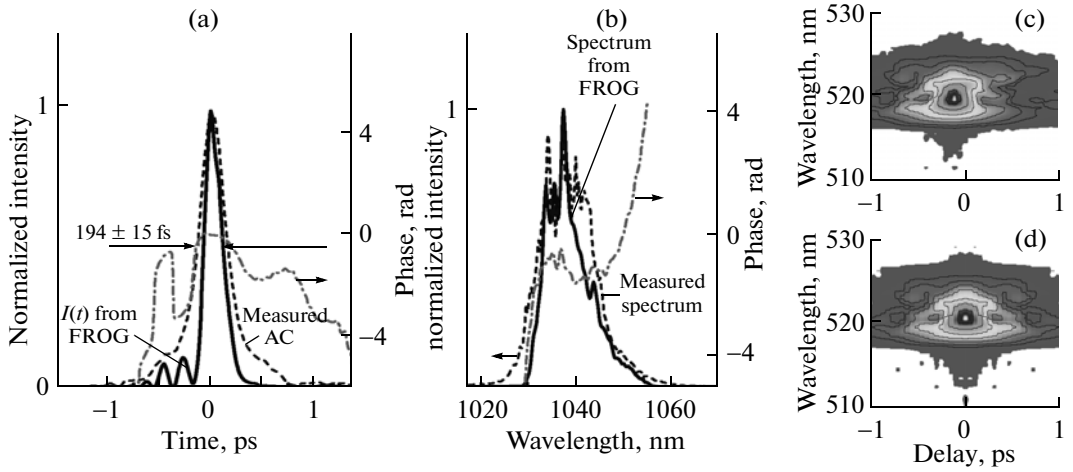

Fig. 4. SHG FROG characterization of the recompressed monolithic YDFA output: (a) retrieved temporal pulse profile and temporal phase and measured autocorrelation function; (b) measured and retrieved spectra together with the spectral phase. (c) Measured and (d) retrieved SHG FROG traces. The pulses are stretched in 480 m of PM SMF.

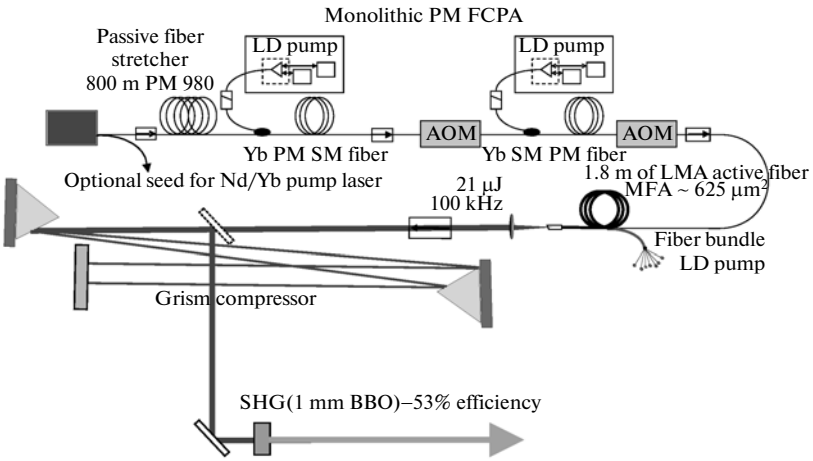

Fig. 5. Experimental layout of the monolithic fiber CPA with 800 m of PM SMF as stretcher unit and ~1.8 m of PLMA-YDF-30/250-HI from Nufern as active medium for the last amplification stage.

figuration, we measured the SHG FROG traces for different pulse energies.

In Fig. 6 the area under the curve of the retrieved pulses was normalized in order to compare how the pulse quality degrades with increasing pulse energy. For these measurements the prism compressor was optimized to achieve the best pulse compressibility at 25 μJ pulse energy. As can be seen from the graph at this energy level the pulse peak intensity decreases because a considerable part of the energy lays in the pulse pedestal. The retrieved phase and temporal pulse profile for a 21 μJ pulse, dechirped down to 187 fs is shown in Fig. 7. This corresponds to a peak power of ~6 MW after compression, which represents to our knowledge the highest peak power demonstrated from a monolithic YDFA. The achieved conversion efficiency of 53% in second harmonic generation illustrates the excellent mode quality and pulse quality of the system.

The YDFA serves both as a potential optical seed (synchronization) source for most Nd and Yb amplifiers operating around 1 μm and as a driver source for the DFG OPA that produces CEP stable near infrared (NIR) seed pulses. In the DFG OPA, the frequency-doubled output of the YDFA is used for the generation of a white light continuum (WLC) seed in bulk sapphire and for its further parametric amplification. CEP stable NIR pulses are produced by generating the difference frequency between the white light continuum and the second harmonic of the YDFA output (see Fig. 1). Using DFG in a 4-mm-long type II BBO between a 1.2 μJ 520 nm pulse and the red wing of the

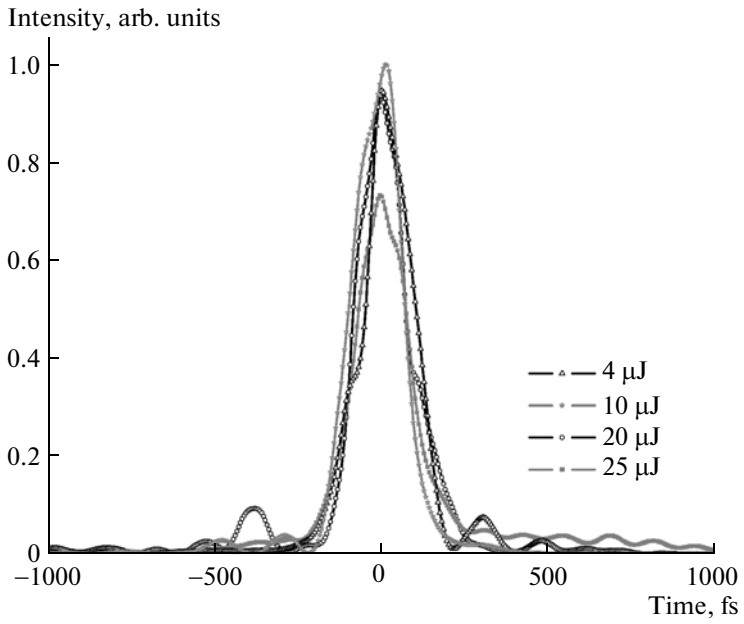

Fig. 6. Retrieved pulse profile of the recompressed pulses alter the final amplification stage of the monolithic YDFA for different output energies. The pulses are stretched in 800 m of PM SMF.

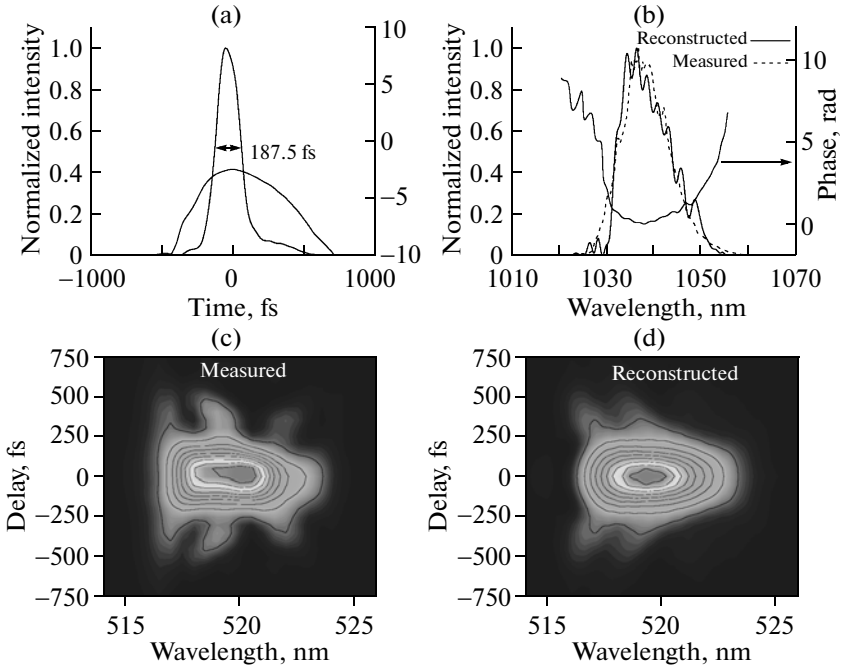

Fig. 7. SHG FROG characterization of the 21 μJ pulses at the output of the monolithic YDFA. The compressed pulse duration is 187 fs FWHM.

white-light continuum pulse generated with a 0.9 μJ 520 nm pulse results in signal and idler pulse energies of up to 80 and 40 nJ, respectively. The NIR pulse is then optionally ×4 amplified in a second OPA (6 mm type II KTP) using the residual 1040 nm fundamental pump light. The tuning properties of the first OPA stage are summarized in Fig. 8. The CEP stability is demonstrated with an f-to-2f interferometer after spectrally broadening the first OPA output pulses in a 55 cm SMF (see Fig. 9). Phase deviations are caused by instabilities of the OPA-arms and the two arms of the f-to-2f interferometer. With the availability of

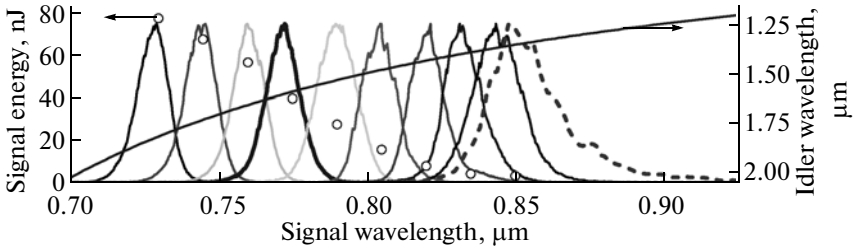

Fig. 8. OPA performance. Tunability of 1st stage OPA (4-mm type BBO seeded with 520-nm-generated white light from a 5-mm-thick sapphire plate.

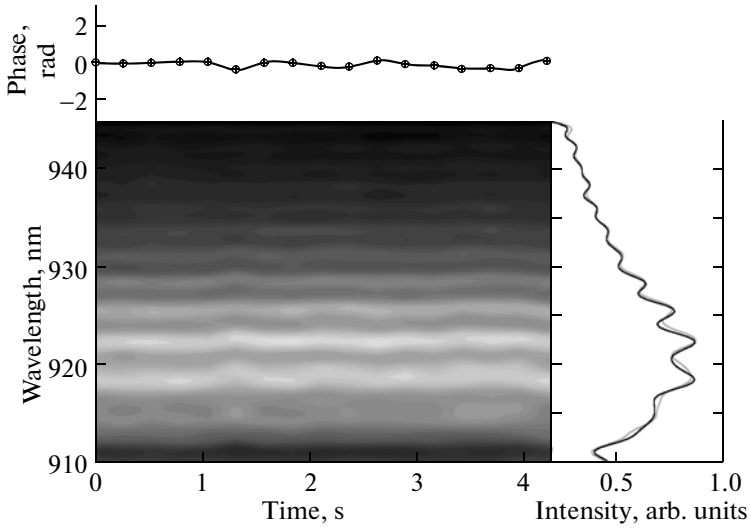

Fig. 9. Measured phase stability with an f-to-2f interferometer after broadening the spectrum of the idler pulses from the first OPA stage in a 55 cm SMF.

higher pulse energy from the monolithic YDFA we expect to considerably improve the CEP stable OPA throughput.

3. CONCLUSIONS

We have demonstrated a monolithic YDFA in which pulse fidelity is preserved by weakening the nonlinear effects in the system via substantially stretching the seed pulses and by using highly doped active fibers as amplifying media. Appropriately choosing the seed source is of key importance for producing high quality pulses. When using an standard ANDi oscillator for seeding the amplifier, poor quality pulses are produced even at lower amplification levels. By using a similariton type oscillator cleaner pulses can be produced. The presented monolithic YDFA delivers up to 21 μJ pulses that can be recompressed to 187 fs pulses. We have also shown that such a turn-key alignment free system can be used for driving DFG CEP stable OPA systems and represents a good alternative to its solid state ytterbium doped counterparts.

ACKNOWLEDGMENTS

This work has been supported by the Austrian Science Fund (FWF), grants U33-N16 and F1619-N08 and by the Austrian Research Promotion Agency (FFG), grant Eurostars 4319. We are grateful to A. Zheltikov for helpful discussions and to K. Regelskis for technical support. A.F. acknowledges support from a Hertha Firnberg Fellowship by FWF (project T420-N16).

REFERENCES

1. S. Hädrich, S. Demmler, J. Rothhardt, C. Jocher, J. Limpert, and A. Tünnermann, Opt. Lett. **36**, 313 (2011).
2. M. E. Fermann and I. Hartl, Laser Phys. Lett. **6**, 11 (2009).
3. O. D. Mücke, D. Sidorov, P. Dombi, A. Pugzlys, A. Baltuska, S. Alisauskas, V. Smilgevicius, J. Pocius, L. Giniunas, R. Danielius, and N. Forget, Opt. Lett. **34**, 118 (2009).

4. A. Fernández, L. Zhu, A. J. Verhoef, D. Sidorov-Biryukov, A. Pugzlys, A. Baltuska, K.-H. Liao, Ch.-H. Liu, A. Galvanauskas, S. Kane, R. Holzwarth, and F. O. Ilday, Opt. Lett. **34**, 2799 (2009).
5. G. P. Agrawal, *Nonlinear Fiber Optics*, 4th ed. (Academic, Boston, 2007).
6. H. Yu, J. Zhou, X. Wushouer, P. Yan, and M. Gong, Laser Phys. Lett. **6**, 653 (2009).
7. J. Limpert, A. Liem, M. Reich, T. Gabler, H. Zellmer, A. Tünnermann, S. Unger, S. Jetschke, and H.-R. Müller, Opt. Lett. **26**, 1840 (2001).
8. C. Ye, P. Yan, L. Huang, Q. Liu, and M. Gong, Laser Phys. Lett. **4**, 376 (2007).
9. L. Kuznetsova and F. W. Wise, Opt. Lett. **32**, 2671 (2007).
10. F. Röser, D. Schimpf, O. Schmidt, B. Ortaç, K. Rademaker, J. Limpert, and A. Tünnermann, Opt. Lett. **32**, 2230 (2007).
11. F. Röser, T. Eidam, J. Rothhardt, O. Schmidt, D. N. Schimpf, J. Limpert, and A. Tünnermann, Opt. Lett. **32**, 3495 (2007).
12. L. Kuznetsova, F. W. Wise, S. Kane, and J. Squier, Appl. Phys. B **88**, 515 (2007).
13. H. Kalaycioglu, B. Oktem, C. Senel, P. P. Paltani, and F. Ö. Ilday, Opt. Lett. **35**, 959 (2010).
14. P. P. Jiang, D. Z. Yang, J. X. Wang, T. Chen, B. Wu, and Y. H. Shen, Laser Phys. Lett. **6**, 384 (2009).
15. A. Chong, J. Buckley, W. Renninger, and F. Wise, Opt. Express **14**, 10095 (2006).
16. A. Chong, W. Renninger, and F. W. Wise, J. Opt. Soc. Am. B **25**, 140 (2008).